

Hydrogel-Based 3D Model of Patient-Derived Prostate Xenograft Tumors Suitable for Drug Screening

Eliza L. S. Fong,[‡] Mariane Martinez,[†] Jun Yang,[§] Antonios G. Mikos,[‡] Nora M. Navone,[§] Daniel A. Harrington,[†] and Mary C. Farach-Carson^{*,†,‡}

[†]Departments of Biochemistry and Cell Biology and [‡]Bioengineering, Rice University, Houston, Texas 77005, United States

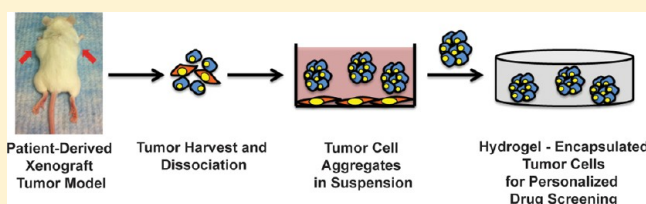
[§]Department of Genitourinary Medical Oncology, University of Texas MD Anderson Cancer Center, Houston, Texas 77030, United States

S Supporting Information

ABSTRACT: The lack of effective therapies for bone metastatic prostate cancer (PCa) underscores the need for accurate models of the disease to enable the discovery of new therapeutic targets and to test drug sensitivities of individual tumors. To this end, the patient-derived xenograft (PDX) PCa model using immunocompromised mice was established to model the disease with greater fidelity than is possible with currently employed cell lines grown on tissue culture plastic.

However, poorly adherent PDX tumor cells exhibit low viability in standard culture, making it difficult to manipulate these cells for subsequent controlled mechanistic studies. To overcome this challenge, we encapsulated PDX tumor cells within a three-dimensional hyaluronan-based hydrogel and demonstrated that the hydrogel maintains PDX cell viability with continued native androgen receptor expression. Furthermore, a differential sensitivity to docetaxel, a chemotherapeutic drug, was observed as compared to a traditional PCa cell line. These findings underscore the potential impact of this novel 3D PDX PCa model as a diagnostic platform for rapid drug evaluation and ultimately push personalized medicine toward clinical reality.

KEYWORDS: Patient-derived xenograft, hydrogel, tumor, drug, prostate cancer



INTRODUCTION

Following a clinically predictable progression pattern, advanced prostate cancer (PCa) metastasizes to distant organs, with a striking predisposition for bone.¹ Despite a decreasing overall mortality rate for PCa patients, survival time remains significantly reduced with metastatic disease.² The development of effective treatments has been hindered, in part, by the lack of cell lines and/or xenograft models that accurately recapitulate the complex metastatic microenvironment.^{2,3} Without appropriate models to reflect the disease, mechanistic studies to accurately elucidate the players involved in PCa progression in bone have been difficult to implement, impeding the development of clinically effective therapeutics targeted to bone metastases.²

Some of the more commonly used PCa cell lines (e.g., PC-3 and DU-145) offer convenience to investigators because they adhere well to tissue culture plastic and therefore are amenable to high throughput screening of drug libraries. However, these same cell lines, when inoculated in bone, generate a largely osteolytic response, in contrast to the predominantly osteoblastic nature of the native human disease. To more accurately model the disease, we have employed the LNCaP cell line progression series (LNCaP, C4, C4-2, and C4-2B), with C4-2B cells forming osseous lesions in bone.⁴ However, we and other investigators continue to search for PCa cell models with greater fidelity to the disease that will foster the

translation of preclinical findings into the clinic, particularly to satisfy the need to identify new treatments that will eradicate PCa metastases growing in bone.

To address the need for the highest-possible fidelity in PCa cell sources, patient-derived xenograft (PDX) models have been established for the preclinical investigation of various aspects of PCa biology including angiogenesis, identification of castrate-resistant stem-like cells, and effect of anti-androgen therapies.^{5–8} PDX models are generated when tumor tissue from the patient is surgically resected and engrafted directly into immunocompromised mice.⁹ Tumors are subsequently maintained solely in vivo via mouse-to-mouse passage, requiring both careful monitoring of the tumor burden and labor intensive animal transfers.⁹ Through serial passaging in mice and the absence of any in vitro manipulation, PDX tumors remain biologically stable, preserving much of the molecular, genetic, and histological features as well as heterogeneity of the original tumor.⁵ However, given the high costs of animal maintenance, lengthy latency period following engraftment,

Special Issue: Engineered Biomimetic Tissue Platforms for in Vitro Drug Evaluation

Received: January 28, 2014

Revised: April 14, 2014

Accepted: April 17, 2014

Published: April 29, 2014

variable engraftment rates, and rare access to patient tissue specimens, PDX in vivo models are generally not yet widely employed in cancer research.⁹ Most notably, given the poor viability exhibited when grown in vitro under standard tissue culture conditions, it is extremely challenging to culture PDX bone metastatic PCa cells for any brief ex vivo manipulation needed to conduct controlled mechanistic studies in vivo.

Mirroring the in vitro behavior of PDX prostate tumors, PCa cell lines belonging to the LNCaP series also adhere poorly to two-dimensional (2D) tissue culture surfaces, precluding them from use in standard drug screening platforms.¹⁰ To circumvent this problem, our laboratory recently demonstrated the feasibility of using three-dimensional (3D) hyaluronan (HA)-based hydrogel systems to support the growth and viability of these PCa cell lines for mechanistic studies and drug testing.^{10–12} While the commonly employed human tumor spheroid model is an alternative to culturing these poorly adherent cells, hydrogel encapsulation provides the means to fully recapitulate the tumor microenvironment with precise, tunable control over architectural and mechanical cues and/or critical cell–extracellular matrix interactions, depending on the type of material used.¹³ Specifically, as a ubiquitous component of the bone marrow where bone metastatic PCa cells reside, HA plays an active role in regulating several biological processes, including tumorigenesis, strongly justifying its use as an extracellular matrix analogue for culturing bone metastatic tumor cells in vitro.¹⁴

On the basis of the suitability of HA-based hydrogel systems for the culture of PCa cell lines, we hypothesized that these systems would similarly support the viability of PDX PCa cells in vitro. Hence, in the present study, we developed a novel protocol to encapsulate PDX PCa cells within 3D HA-based hydrogels and examined tumor cell morphology, viability, proliferative capacity and phenotype. We also tested the potential of this 3D PDX PCa model as a diagnostic platform for evaluating rapid patient-specific drug response, a significant advance toward achieving a more personalized therapeutic regimen.

MATERIALS AND METHODS

Materials. Phenol red-free Dulbecco's Modified Eagle Medium/Nutrient Mixture F-12 (DMEM/F-12), T-medium, penicillin/streptomycin, trypsin-EDTA, L-glutamine, LIVE/DEAD viability/cytotoxicity kit, and Quant-iT PicoGreen dsDNA Assay kit were obtained from Life Technologies (Grand Island, NY). Fetal bovine serum (FBS) was obtained from Atlanta Biologicals (Flowery Branch, GA). Phosphate buffered saline (PBS) was obtained from Lonza (Walkersville, MD). ACCUMAX was obtained from eBioscience (San Diego, CA). Thiol-modified HA (HA-SH, Glycosil, average M_w = 240 kDa, degree of thiolation = 1 $\mu\text{mol/mg}$ HA-SH) and poly(ethylene glycol)-diacrylate (PEG-DA, Extralink, average M_w = 3350 Da) were obtained from BioTime Inc. (Alameda, CA). This HA-SH/PEG-DA hydrogel system previously has been characterized extensively.^{15–17} Docetaxel was obtained from Selleck Chemicals (Houston, TX). DMSO, L-cysteine, and papain papaya latex were obtained from Sigma-Aldrich (St. Louis, MO). Primary antibodies used were human-specific anti-nuclei antibody from Millipore (MAB1281, Billerica, MA), anti-androgen receptor from Santa Cruz Biotechnology (sc-816, Dallas, TX), anti-cleaved caspase-3 from Cell Signaling Technology (NB110–89717, Danver, MA), and anti-Ki-67 from Novus Biologicals (#9664S, Littleton, CO). Sylgard 184

poly(dimethylsiloxane) (PDMS) elastomer kit was from Dow Corning (Midland, MI).

PDX Cell Preparation. MDA PCa 183 and MDA PCa 118b cells were routinely maintained as subcutaneous tumors in CB-17 SCID mice (Charles River). All experiments for the propagation of PDX tumors in mice were conducted under IACUC approval from the University of Texas MD Anderson Cancer Center. The MDA PCa 183 xenograft was derived from androgen-dependent prostate carcinoma, whereas the MDA PCa 118b was derived from androgen receptor-negative castrate-resistant prostate carcinoma.¹⁸ For this study, MDA PCa 183 and MDA PCa 118b PDXs of passage 12 and 8 respectively, were used. On the day of harvest, the animal hosts were sacrificed by cervical dislocation. Tumor specimens were removed immediately, rinsed six times with PBS, minced with a scalpel blade, and digested with ACCUMAX enzymatic solution for 15 min at 37 °C. The enzyme solution was inactivated with FBS, the resultant tumor slurry was filtered through a 70 μm cell strainer, and the filtrate was centrifuged. The supernatant was removed, the resulting cell pellet was resuspended, and a cell count was performed.

PDMS Mold Preparation. Custom-made PDMS molds were made by mixing Sylgard 184 elastomer and cross-linker 10:1 (v/v) according to manufacturer's instructions. The liquid silicone solution was centrifuged at 4 °C/3000 rpm/5 min to remove bubbles and poured into a square aluminum frame with a 1.5 mm-thick spacer. Slabs were cured in a Carver press at 100 °C for 45 min. An X-660 automated CO₂ laser cutter (Universal Laser Systems, Scottsdale, AZ) was used at 2.5% speed and 60% power to cut the slabs into 24 × 60 mm rectangles with multiple 6 mm diameter cylindrical cavities. The resultant molds were steam-autoclaved before each use and were sealed onto sterile glass slides before being employed as molds for hydrogel fabrication. Each cylindrical cavity could hold approximately 50 μL of hydrogel.

Prior to PDX tumor culture, HA-SH and PEG-DA were solubilized at 10 and 20 mg/mL, respectively, in degassed water per the manufacturer's instructions. The solutions were mixed at 4:1 (v/v) ratio, 35 μL of the combined solution was placed in each cavity of the silicone molds, and the mixture was allowed to cross-link for 1 h at 37 °C. The bottom layer of acellular hydrogel served as a "cushion layer" to prevent cell clusters from settling out of the cell–hydrogel construct during culture.

PDX Tumor Culture. Following tumor harvest, unsorted cells from the processed tumors were plated on 6-well plates at densities determined to yield hydrogel constructs with 150,000 and 300,000 encapsulated MDA PCa 183 and MDA PCa 118b cells respectively, per construct. MDA PCa 183 and MDA PCa 118b cells were cultured in DMEM/F-12 supplemented with 10% and 30% (v/v) FBS, respectively, in the presence of 100 U/mL of penicillin and 100 $\mu\text{g/mL}$ of streptomycin. Tumor cells then were incubated at 37 °C with 5% CO₂ for 2 days, after which tumor cell aggregates that formed in suspension from all wells were collected into sterile 15 mL tubes and gently centrifuged. Supernatant was removed from each tube, and the remaining cell pellets were resuspended in complete DMEM/F-12 medium, combined, and split into microcentrifuge tubes and centrifuged again. Notably, as these cells form clusters in suspension, we could not perform cell counts immediately prior to encapsulation. Instead, cell counting for the preparation of hydrogel constructs was performed at the step of 2D culture in 6-well plates (immediately after the tumors were dissociated). The resulting cell pellets then were resuspended in solutions of

HA-SH and PEG-DA (4:1 v/v) as described above, and 25 μL of the cell-hydrogel suspension was immediately pipetted into each mold cavity, over the 35 μL cushion layer of cross-linked HA-SH/PEG-DA. Seeded hydrogels were returned to the incubator for 45 min, then immersed in cell culture medium and incubated overnight. The following day, each mold cavity was scored with a 26-gauge needle, cell-hydrogel constructs were transferred into 24-well plates and submerged in culture medium. Medium was exchanged every other day.

Culture of Established Cell Lines. The C4-2B bone metastatic PCa cell line was maintained in T-medium containing 5% FBS (v/v) and 2 mM L-glutamine in the presence of 100 U/mL of penicillin and 100 $\mu\text{g}/\text{mL}$ of streptomycin. For the docetaxel drug study, 50,000 cells were encapsulated within HA-SH/PEG-DA as described above for the PDX tumors. A lower cell density was used for the cell line because high-density culture was associated with poor cell viability (data not shown).

Drug Treatment. Cell-hydrogel constructs ($n = 3$) were maintained for 2 days before treatment with docetaxel for 3 days. Docetaxel was diluted in dimethyl sulfoxide (DMSO) such that the final concentration of DMSO was 1% (v/v) in complete medium across all drug concentrations. Vehicle controls were treated with DMSO only.

Imaging. Morphology of the cells encapsulated within the hydrogel was monitored by differential interference contrast microscopy at days 1, 3, 5, and 7 postencapsulation using a Nikon Eclipse TE300 inverted microscope and NIS Elements software (Nikon Instruments, Melville, NY). Fluorescently labeled samples were imaged using a Nikon A1-Rsi confocal microscope and images processed using the Nikon NIS-Elements AR software (Nikon Instruments, Melville, NY).

Cell Viability. Cell viability was assessed using the LIVE/DEAD viability/cytotoxicity kit as per the manufacturer's instructions. Briefly, cell-hydrogel constructs at the designated time-points were incubated in 2 μM calcein-AM and 4 μM ethidium homodimer-1 in PBS for 30 min at 37 °C before confocal imaging.

DNA Quantification. Cell-hydrogel constructs ($n = 3$ or 4) were collected into individual microcentrifuge tubes at the designated time-points, flash-frozen using liquid nitrogen, and stored at -80 °C. Frozen samples then were lyophilized overnight and digested in PBE buffer (0.10 M Na_2HPO_4 and 0.010 M Na_2EDTA in demineralized water at pH 6.5) containing 125 $\mu\text{g}/\text{mL}$ papain in the presence of 14.5 mM L-cysteine at 65 °C overnight.¹⁹ The digested samples then were sonicated using a probe sonicator, and the liquid supernatant was assayed using the Quant-iT PicoGreen dsDNA quantification assay as per the manufacturer's instructions. Acellular hydrogel constructs served as blank controls. Excitation and emission wavelengths of 485 and 528 nm, respectively, were used to measure the fluorescence (FLx800 fluorescence microplate reader; BioTek Instruments). Lambda DNA was used to standardize the samples against a calibration curve.

Immunocytochemistry. Cell-hydrogel constructs were washed with PBS and fixed with 4% (v/v) paraformaldehyde for 10 min at room temperature. After fixation, constructs were washed with PBS and stored at 4 °C until staining. Constructs were immersed in 0.2% (v/v) Triton X-100 for 5 min at room temperature to permeabilize cells, then blocked with 500 μL of 3% (w/v) BSA and 0.2% Triton X-100 in PBS at 4 °C overnight. All antibodies were diluted at 1:200 in 3% BSA and 0.2% Triton-X-100 in PBS. Antibody staining was performed

using 200 μL of the mixed solution to each sample, which were placed on a rocking platform shaker at 4 °C overnight. Samples were washed with PBS before adding fluorophore-labeled secondary antibodies directed against the appropriate host. Secondary antibodies were diluted 1:500 in 3% BSA and 0.2% Triton-X-100 in PBS, and 200 μL of that solution was added to each sample. Samples then were placed on a rocking platform shaker at 4 °C overnight. Samples were washed with PBS to remove unbound secondary antibodies. DAPI (5 $\mu\text{g}/\text{mL}$) was added to each sample at room temperature for 5 min. When phalloidin was used, it was diluted 1:20 in PBS, and 100 μL of that mixture was added to each sample for 15 min. Samples then were washed with PBS for 5 min. All immunofluorescence images were captured with a Nikon A1-Rsi confocal microscope.

Statistical Analysis. Data are expressed as mean \pm SEM. Statistical analysis was performed using the Tukey's HSD test. Differences were considered significant at $p < 0.05$.

RESULTS

Generation of 3D PDX Tumoroids Encapsulated within HA-SH/PEG-DA Hydrogels. In initial experiments, following tumor digestion, we encapsulated the entire PDX cell population directly into hydrogels. When we did so, a large number of dead cells was transferred to the hydrogels as observed after 1 day in 3D culture (data not shown). These dead cells likely were generated during the tumor harvest and digestion, and also contain mouse-derived cells that die immediately within the hydrogels. As the presence of high numbers of dead cells would complicate any biochemical assays that were envisioned, we sought to develop an alternative procedure designed to encapsulate cells with high viability (Figure 1A).

In optimizing the culture conditions for the PDX PCa cells, we observed that most of the MDA PCa 183 and MDA PCa 118b PCa cells that had undergone mechanical and enzymatic digestion and been plated onto 6-well plates formed multicellular aggregates in suspension after 2 days in culture, presumably reflecting their characteristic poor adherence onto tissue culture plastic (Figure 1B). Additionally, during this period, we noted that a population of cells in the tumor slurry (shown in red in Figure 1A) adhered to the tissue culture plastic surface. Leveraging this phenomenon, we collected the aggregates in suspension (leaving behind the adherent cells) and found that the process of gentle centrifugation resulted in the removal of dead cells. Given that the MDA PCa 183 and MDA PCa 118b tumors were grown as subcutaneous tumors in mice, they carry along with them a subpopulation of mouse-derived cells in addition to the human PCa cells. Indeed, we found that among the poorly adherent PCa cells that formed multicellular aggregates in suspension after 2 days on tissue culture plastic, the cells that had adhered stained positive for vimentin (Figure 1C). Henceforth, we employed this pre-encapsulation 2D culture method, which not only removes dead cells, but also enriches the PDX tumor population via the depletion of mesenchymal cells. A summary of the process used to form 3D PDX tumoroids within the HA-SH/PEG-DA hydrogel is illustrated in Figure 1A.

Cellular Composition of 3D Tumoroids. In the first week after encapsulation, MDA PCa 183 cells were maintained as large tumoroids with most having diameters between 60–100 μm . MDA PCa 118b cells were maintained as smaller tumoroids, typically smaller than 60 μm in diameter (Figure

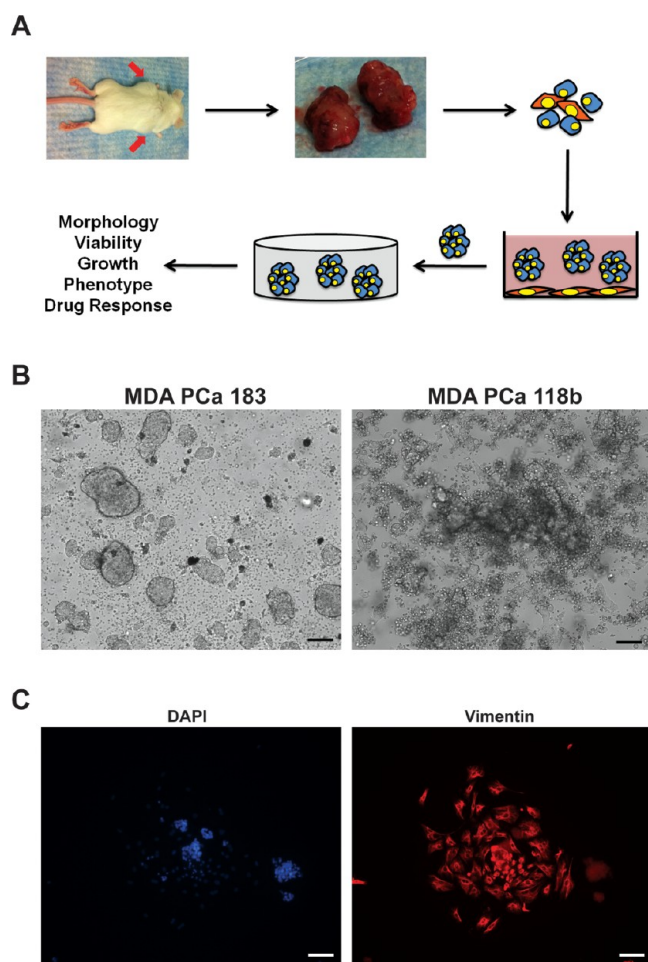


Figure 1. Three-dimensional hydrogel platform for PDX culture. (A) MDA PCa 183 and MDA PCa 118b PDX tumors (indicated by red arrows) that were grown subcutaneously in SCID mice were harvested, then mechanically and enzymatically digested. The tumor slurry was subsequently plated onto 6-well plates and cultured for 2 days during which the majority of mouse-derived cells (red) attached. The resulting tumor aggregates that formed (blue) then were encapsulated within HA-SH/PEG-DA hydrogels and cultured for up to 14 days. Cancer cells = blue, mouse fibroblasts = red. (B) Dissociated tumor cells plated on tissue culture plastic for 2 days formed multicellular clusters in suspension with other cell types adhering to the plastic surface. (C) Mixture of DAPI-stained (blue) cells within tumoroids and adherent cells after 2 days in culture. Adherent cells stained positive for vimentin (red). Scale bars = 100 μ m.

2A and Supplementary Figure 1). Cells in tumoroids were in close contact in multicellular clusters, observed via staining with phalloidin for F-actin (Figure 2B). To demonstrate that human PCa cells comprise the 3D PDX tumoroids, we stained the encapsulated cells for epithelial cell adhesion molecule (EpCAM), an established marker for epithelial cells. As expected, both the MDA PCa 183 and MDA PCa 118b 3D PDX tumoroids stained positive for EpCAM (Figure 2C), indicating that the tumoroids form from self-sorting epithelial cells despite the presence of mesenchymal cells in the original xenograft tumors. Additionally, we also confirmed this by probing for the human-specific anti-nuclei antibody and found that the majority of cells within the tumoroids stained positive (data not shown), indicating that the 3D PDX tumoroids form from largely human cells. Next, we asked if the PCa cells in tumoroids retained their androgen receptor activation status.

Probing specifically for the androgen receptor, we found that while the androgen receptor was mainly localized in the nucleus of cells in the MDA PCa 183 tumoroids, nuclear localization of the receptor was not observed in the MDA PCa 118b cells as would be expected in vivo.

Viability and Growth of 3D PDX Tumoroids.

Encapsulation of the nonadherent tumoroids into HA-SH/PEG-DA hydrogels maintained cell–cell contacts for at least 2 weeks in culture. Given that these PDX PCa tumors exhibit poor viability in vitro on 2D, we next investigated whether the encapsulated PDX tumoroids remained viable within the hydrogels over time using the LIVE/DEAD viability/cytotoxicity assay. As shown in Figure 3, cells in both the MDA PCa 183 and MDA PCa 118b tumoroids were predominantly viable at days 1, 5, and 14. Remarkably, PDX cells had the highest survival when they had formed large clusters with other cells. Dead or dying cells in each hydrogel were observed to be one of two types: either single cells that had not aggregated with other cells to form multicellular clusters or cells on the periphery of each cluster (particularly prominent in Figure 3B, day 14). Beyond viability, to establish if the 3D PDX tumoroids demonstrate tumor growth characteristics necessary for the model to serve as a drug-testing platform, particularly for drug candidates that target actively dividing cells, we monitored their growth over 1 week in culture, using DNA content as a surrogate measure of cellularity. Notably, the overall cellularity of the MDA PCa 118b constructs was lower than that of the MDA PCa 183 because the MDA PCa 118b cells formed smaller clusters, therefore the retrieval of cells for hydrogel encapsulation was less efficient than from the MDA PCa 183 cultures. This is apparent from the finding that even though a higher theoretical seeding density (150,000 and 300,000 cells per construct for MDA PCa 183 and 118b, respectively) was employed for the MDA PCa 118b constructs, the average initial DNA content of the MDA PCa 118b constructs still was lower than that of the MDA PCa 183 constructs (day 1, Figure 4A). In analyzing the cellularity of the 3D PDX constructs over time, while DNA content remained constant with no significant difference over time for the MDA PCa 183 tumoroids, there was a significant decrease in cellularity for the MDA PCa 118b from day 1 to 5, after which an increase in cellularity was observed (Figure 4A). Probing the 3D PDX tumoroids for Ki-67 and cleaved caspase-3, markers of proliferation and apoptosis, respectively, we found that differences in the proportion of proliferative and apoptotic cells at day 5 in culture was not apparent for either MDA PCa 183 or 118b (Figure 4B,C).

Response of 3D PDX Tumoroids to Docetaxel. Having demonstrated that the encapsulated 3D PDX tumoroids are (1) made up of viable PCa cells, (2) maintain in vivo-like androgen receptor distribution, and (3) are proliferative in the hydrogels, we next determined the suitability of this in vitro platform for drug testing of primary PCa cells. Given the inherent differences in origin between the MDA PCa 118b and MDA PCa 183 PDX models, we hypothesized that they would demonstrate a differential sensitivity to chemotherapeutic drugs. To test this hypothesis, we exposed the 3D MDA PCa 183 and MDA PCa 118b tumoroids to docetaxel, currently part of the first line regimen to treat patients with castrate-resistant metastatic PCa. Surprisingly, we found that not only was there no overall difference in docetaxel sensitivity between the 3D MDA PCa 183 and MDA PCa 118b tumoroids, no significant reduction in cell number was detected within the range of

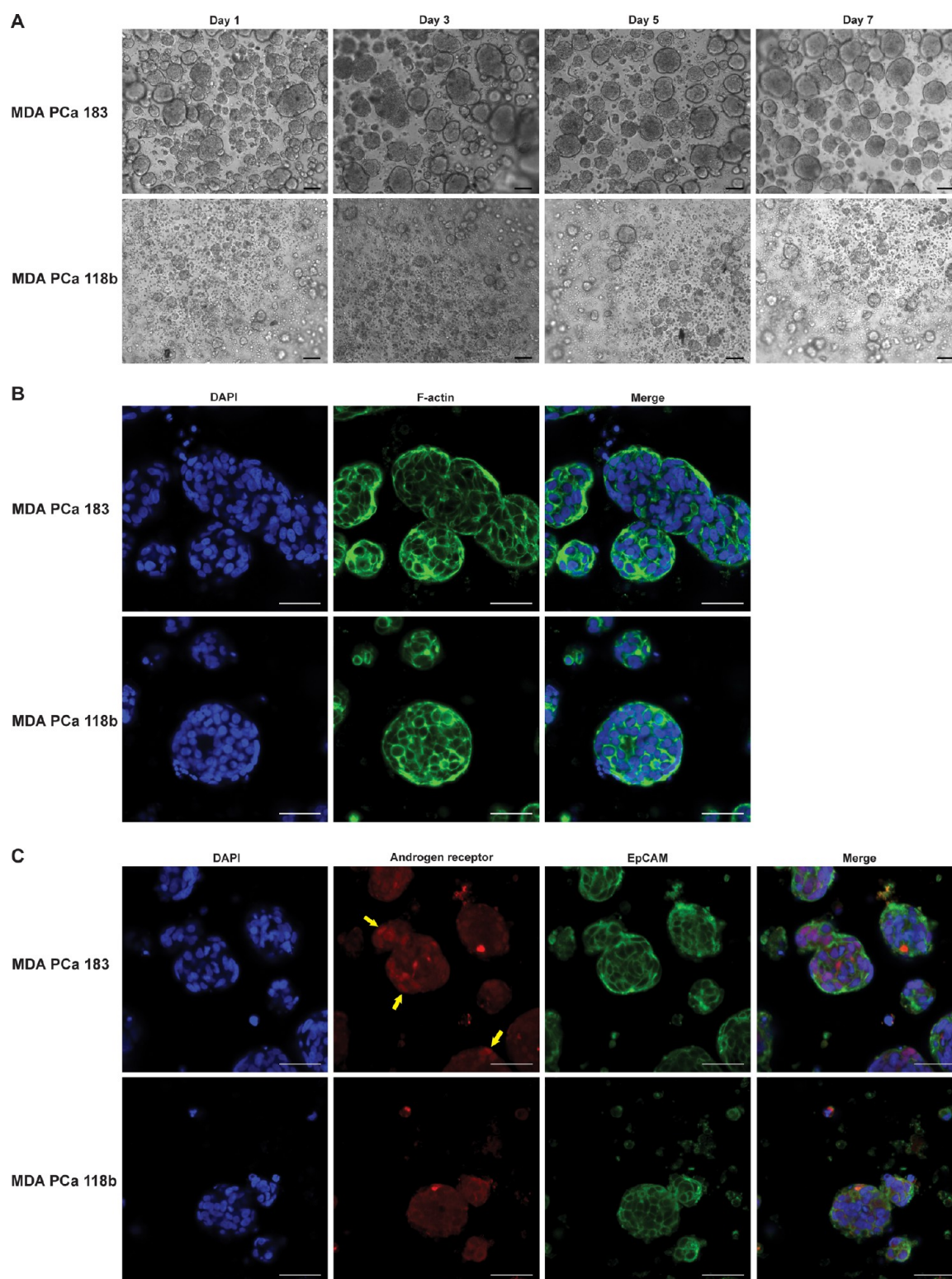


Figure 2. Generation of PDX tumoroids encapsulated within 3D HA-SH/PEG-DA hydrogels. (A) MDA PCa 183 and MDA PCa 118b cells remained as multicellular tumoroids post-encapsulation, over 1 week in culture. Scale bar = 100 μm . (B) Phalloidin-staining reveals degree of multicellularity of tumoroids. Cells were stained with DAPI (blue) or phalloidin (green); a merged image is shown on the right panel. Scale bar = 50 μm . (C) Hydrogel-encapsulated MDA PCa 183 and MDA PCa 118b cells were stained with DAPI (blue), and with antibodies against EpCAM (green) and the androgen receptor (red). While the MDA PCa 183 cells exhibited nuclear localization of the androgen receptor (indicated by yellow arrows), the MDA PCa 118b cells stained negative for nuclear localization of the androgen receptor. Both 3D PDXs expressed EpCAM. Scale bar = 50 μm .

docetaxel concentrations tested for either 3D tumoroid systems (Figure 5A). To confirm these findings, we performed the

LIVE/DEAD viability/cytotoxicity assay and found that cells were largely viable even at the highest docetaxel concentration

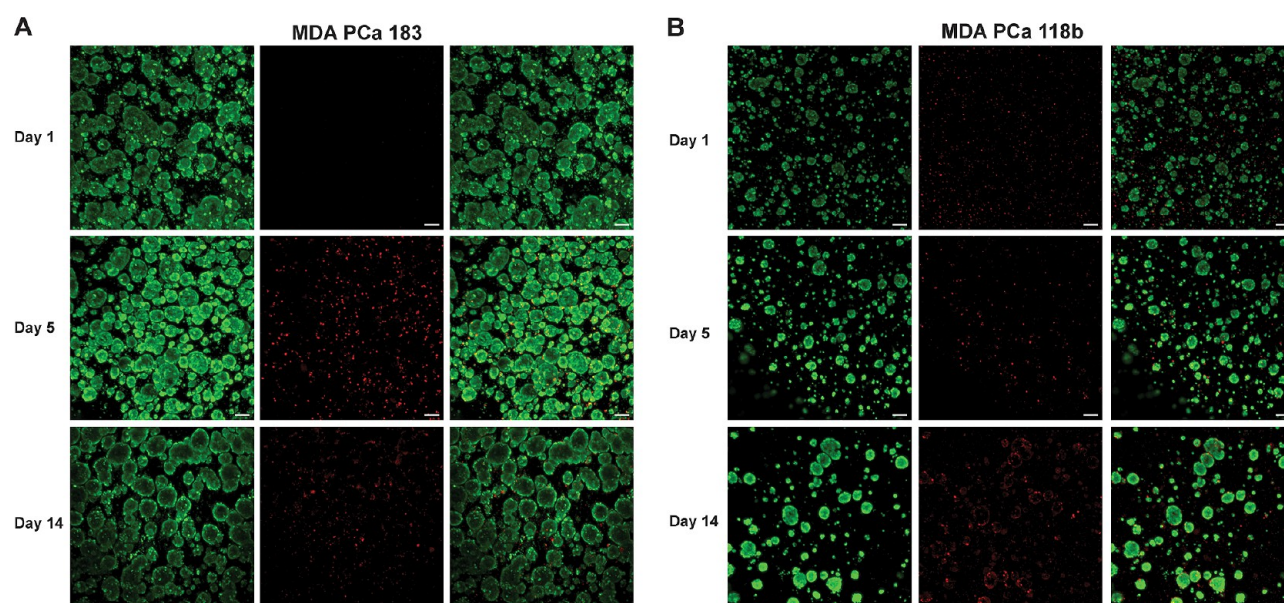


Figure 3. Three-dimensional PDX tumoroids remain viable over time in culture. Panels in (A) and (B) show MDA PCa 183 and 118b after 1, 5, and 14 days in culture, respectively. Cells were stained with calcein-AM (green, left panel) or ethidium homodimer-1 (red, middle panel). The right panel shows a merge of both images. Scale bar = 100 μm .

(Figure 5B). Additionally, there were no apparent differences in the proportion of apoptotic cells as indicated by cleaved caspase-3 staining at the various docetaxel concentrations tested (Supplementary Figure 2). To demonstrate that the lack of cell-kill was cell source-dependent, we similarly exposed hydrogel-encapsulated cells from a bone metastatic prostate cancer cell line, C4-2B, to docetaxel. Interestingly, a significant decrease in cellularity was already apparent between 1 and 10 nM (Figure 5A,B). This finding was corroborated by an observed increase in the proportion of ethidium homodimer-1-stained cells with increasing concentration of docetaxel (Figure 5B). Notably, given that viable C4-2B cells were present at 10,000 nM as observed by calcein-AM staining, it is likely that the decrease in the proportion of calcein-AM-stained C4-2B cells due to drug cytotoxicity could not be clearly discerned when compared to controls. We also showed that the PDX cells were readily killed with 1 M sodium azide; thus, it was likely not an issue of drug accessing the PCa cells (data not shown).

DISCUSSION

In this study, we assessed a 3D HA-based hydrogel system for the culture of primary PDX bone metastatic PCa tumors, well-known to exhibit poor viability when cultured on tissue culture plastic *in vitro*. Given the ubiquity of HA in the bone marrow extracellular matrix and our previous studies that demonstrated the feasibility of using 3D HA-based hydrogels to culture poorly adherent bone metastatic PCa cell lines, we hypothesized that these biologically active hydrogels would serve as excellent matrices to support the long-term culture of primary PDX PCa tumor tissue *in vitro*.^{10–12}

The inability of bone metastatic PCa cells, whether derived from cell lines or primary PDX tumor tissue, to grow in 2D culture is an established phenomenon that indicates the lack of critical components from the bone microenvironment upon which these highly adapted cells depend. In optimizing the culture conditions for the 3D PDX PCa cells, we found that the cancer cells failed to adhere to tissue culture plastic, as was expected. Instead, these cells aggregated to form multicellular

aggregates in suspension, where the formation of cell–cell contact is a likely mechanism employed by the PCa cells to adapt to the loss of native cell–matrix interactions. Indeed, as proposed by Shen and Kramer, cancer cells are capable of undergoing “synoikis”, a term that was used to describe the avoidance of apoptosis by relying on intercellular adhesions in the absence of cell–matrix interactions.²⁰ Focusing specifically on squamous cell carcinoma cells, the authors demonstrated that E-cadherin-mediated cell–cell contact resulted in the generation of compensatory survival signaling via the epidermal growth factor receptor.²⁰ Interestingly, a similar observation was made by a landmark report by Kondo et al., who showed that sustained E-cadherin-mediated cell–cell interactions were necessary for the survival of primary patient-derived colorectal cancer cells in suspension culture.²¹

In optimizing the culture method for the primary PDX PCa cells, we leveraged the ability of the cancer cells to spontaneously aggregate to form multicellular clusters in suspension as a means to reduce the presence of “contaminant” cells such as dead cells, including those that were originally from the tumor tissue itself (in regions of necrosis) and those that were generated during the process of tumor digestion. We found that the application of gentle centrifugation to retrieve the PCa aggregates in suspension after 2 days on tissue culture plastic was an effective method to separate the PCa cells from dead cells in suspension prior to encapsulation within the hydrogel. Given that the PDX PCa cells were maintained in mice prior to harvest, the cancer cells were also likely “contaminated” with mouse-derived cells (such as blood cells, endothelial cells, or fibroblasts), which consequently introduces a source of heterogeneity and complicates downstream biochemical studies. Furthermore, considering the importance of the tumor microenvironment in influencing tumor behavior, the presence of mouse-derived stroma may confound studies evaluating species-specific stroma-targeting drug candidates, hence making it a major hindrance in current PDX tumor models.⁵ Indeed, while the PCa cells formed aggregates in suspension, a population of cells was consistently observed to

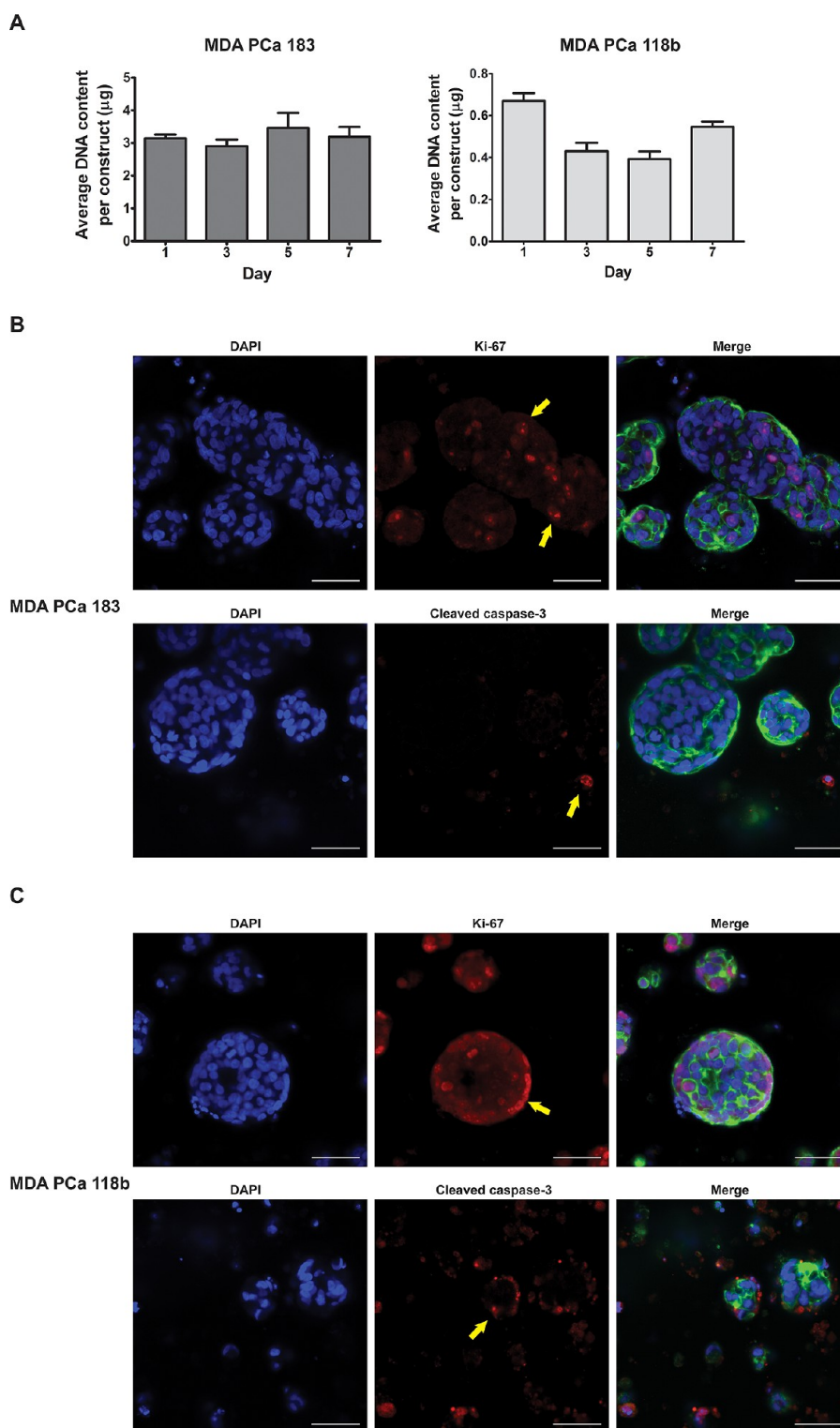
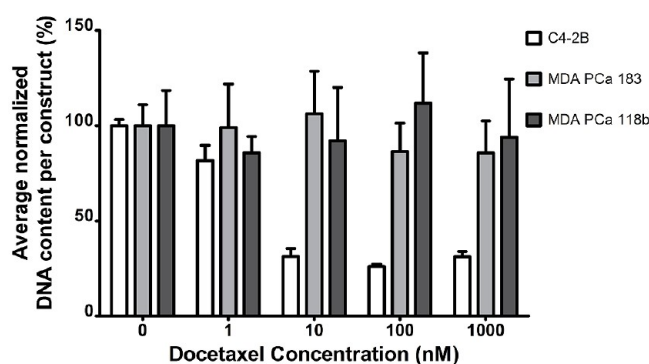


Figure 4. Cellularity is maintained in the 3D PDX constructs over time. (A) Average cellularity of the 3D MDA PCa 183 and 118b constructs over 1 week in culture. Upper panel of (B) and (C) shows the MDA PCa 183 and MDA 118b tumoroids, respectively, stained with DAPI (left panel, blue) and antibodies against Ki-67 (middle panel, red). The right panel shows a merged image where green indicates F-actin. Lower panel of (B) and (C) shows the MDA PCa 183 and MDA PCa 118b tumoroids, respectively, stained with DAPI (left panel, blue) and antibodies against cleaved caspase-3 (middle panel, red). The right panel shows a merged image where green indicates F-actin. Yellow arrows indicate positive staining. Scale bars = 50 μm .

adhere to the tissue culture plastic surface. For example, in MDA PCa 183 cultures, we found that the adherent cells expressed vimentin and originated from mouse tissue (Figure 1C). While further characterization is necessary to determine

the actual yield of the cancer cells, these results, in conjunction with the observation that EpCAM, an epithelial cell marker, was near-ubiquitously expressed in all of the hydrogel-encapsulated PDX clusters (Figure 2C), highly suggest that the pre-

A



B

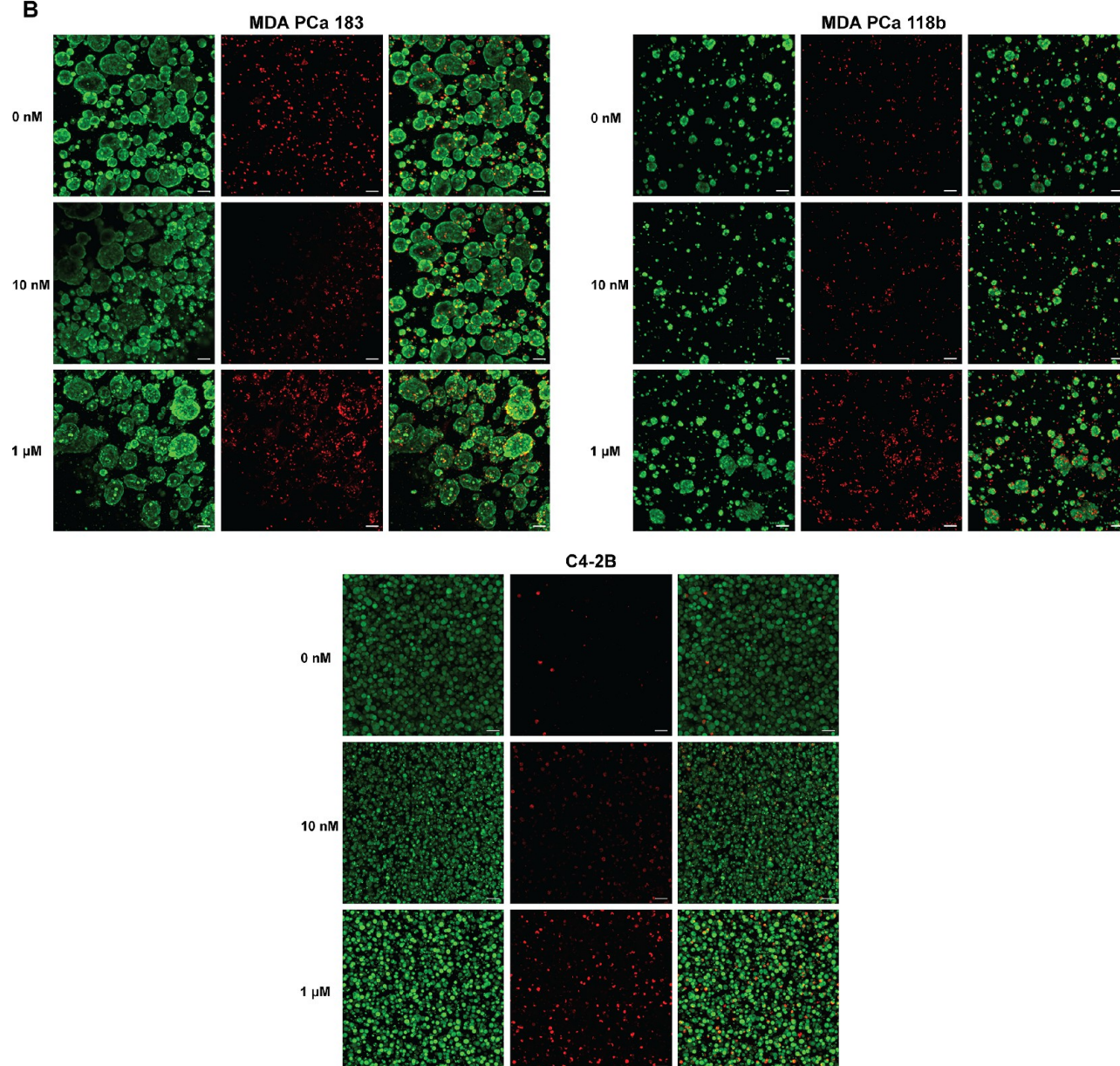


Figure 5. Response of 3D PDX tumoroids to docetaxel. (A) Average cellularity of 3D MDA PCa 183 and 118b constructs after exposure to increasing docetaxel concentrations, compared to the C4-2B cell line, also hydrogel-encapsulated. C4-2B cells exhibited significantly lower resistance to docetaxel as compared to both PDXs ($p < 0.05$). (B) Viability of cells after exposure to 0, 10, or 10,000 nM docetaxel, assessed by calcein-AM staining (green, left panels) and ethidium homodimer-1 (red, middle panels). Right panels show merged images. Scale bars = 100 μm.

encapsulation 2D culture serves as a desirable selective method to generate viable and enriched PDX PCa cells in 3D.

In this study, we optimized the culture of PDX PCa cells in vitro, which to our knowledge is unprecedented. While robust growth was limited by a balance between proliferation and apoptosis, viability of the hydrogel-encapsulated PCa cells was notably well maintained even up to 14 days in culture (Figure 3). Ten to 20% of cells within the 3D PDX tumoroids stained positive for Ki-67 at day 5 in culture (Figure 4B,C), indicating that a subset of cells was still progressing through the cell cycle. Comparing the proportion of proliferative cells within the 3D MDA PCa 118b PDX tumoroids to their in vivo counterparts, we found that our estimate of Ki-67-positive cells is well within the range of that in vivo.²² We are currently modifying the HA-based hydrogel to study the effects of ECM moieties and other cell types on the growth behavior of the PDX PCa tumoroids in 3D culture.

With the shift in focus from traditional chemotherapy to biologically targeted approaches based on a mechanistic understanding of PCa biology, preservation of salient features of the original tumor is a critical criterion in evaluating the success of this culture system as a drug-testing platform. To this end, we probed specifically for the expression of the androgen receptor. The androgen receptor is an important modulator for prostate growth and currently the primary therapeutic target in PCa.²³ Additionally, this nuclear receptor regulates PSA expression, which is used clinically as a biochemical marker to track the progression of PCa and response to therapy.²⁴ Predominantly cytoplasmic in the absence of ligands, ligand binding to the androgen receptor results in conformational changes, nuclear translocation of the ligand-bound receptor, and transcriptional activity.²⁵ Mirroring the in vivo tumor, detection of nuclear androgen receptor in the 3D MDA PCa 183 tumoroids indicates that the HA-SH/PEG-DA hydrogel system is capable of maintaining critical androgen receptor signaling in these androgen-dependent cells. Similarly, nuclear androgen receptor was not observed in the 3D MDA PCa 118b tumoroids as would be expected in in vivo, indicating that these 3D PDX models may have utility as drug-testing platforms evaluating androgen receptor-targeting agents currently under intense clinical investigation.^{18,26}

Drug discovery and screening has historically relied on cancer cell lines, which have generated a wealth of knowledge in cancer biology. However, the dichotomy in drug efficacy between preclinical and clinical testing is increasingly apparent, primarily attributed to the genetic and epigenetic changes that accrue when cells acclimatize to the in vitro culture environment in extended periods of cell culture.⁵ Indeed, Gillet et al. evaluated the multidrug resistance transcriptome of six cancer types and found no correlation between clinical samples and established cell lines, underscoring the need for new in vitro cancer models and primary tumor models.²⁷ Hypothesizing that inherent differences exist between traditional PCa cell lines and PDX PCa tumors, we evaluated the response of the 3D PDX PCa tumoroids (MDA PCa 183 and 118b) to docetaxel and compared their response to the C4-2B bone metastatic prostate cancer cell line. Docetaxel is a microtubule stabilizer and is currently part of the first-line standard treatment for metastatic castrate-resistant PCa.²⁸ We found that despite the differences between the MDA PCa 183 and 118b cells in patient origin, their overall drug sensitivity to docetaxel was similar. Given that both PDX-derived cultures showed a low number of proliferating cells and that docetaxel targets actively dividing

cells, it thus was unsurprising that both demonstrated similar resistance to the drug in 3D culture. However, interestingly, the 3D PDX PCa cells exhibited a significantly higher resistance to the drug as compared to the C4-2B cells. It is unlikely that the increased resistance is due to impaired diffusion of the drug into the hydrogel since it demonstrated clear efficacy against the hydrogel-encapsulated C4-2B cells. While results from this drug study are promising, studies are ongoing to establish clinical relevance and understand the mechanisms underlying this difference.

With the increasing awareness that irreversible biological changes occur when conventional cell lines are established in vitro, beyond prostate cancer, there is general shift toward the use of PDX tumor models for cancer research.^{5,21,27,29–31} However, their utility depends on the ability to manipulate the tumor cells ex vivo prior to implantation.⁹ Given the alterations in biological properties associated with 2D culture, a few groups have taken steps to optimize methods to reliably grow primary tumor cells in 3D. One such example is in colorectal cancer, where it has been shown that primary colorectal cancer cells can be cultured as 3D spheroids or colospheres in vitro, enabling the manipulation of the cancer cells before engraftment in vivo for controlled studies.^{21,32} In our current study, we demonstrate for the first time that primary bone metastatic PCa cells can similarly be cultured in vitro with the use of a 3D HA-based hydrogel system. Lastly, this 3D PDX model may ultimately be adapted to a rapid and high throughput platform for assessing drug efficacy, rational drug combinations, and development of predictive biomarkers for novel targeted therapies, while reducing the need for low throughput animal hosts. As an example, we showed here that 3D PDX PCa cells exhibited an increased resistance to docetaxel as compared to a standard cell line commonly used in PCa research. Studies are ongoing to assess the clinical relevance of this finding. Ultimately, it is envisioned that the use of 3D PDX models may greatly accelerate the advancement of novel drug candidates together with predictive biomarkers that enable patient selection when translated into early phase clinical trials.⁵

■ CONCLUSIONS

On the basis of previous success culturing bone metastatic PCa cell lines using 3D HA-based hydrogels, we demonstrate for the first time that “never in 2D” PDX PCa tumors can be cultured in vitro and maintained for at least 2 weeks. The resulting hydrogel-encapsulated 3D PDX tumoroids retained viability, proliferative capacity, and the androgen receptor expression, indicating that this novel 3D PDX model may serve as a valuable platform for drug development. While it has yet to be tested, this system promises the possibility of culturing tumor tissue directly from the patient for rapid drug screening, thereby eliminating the “middle mouse” and its associated problems, a major leap toward personalized medicine.

■ ASSOCIATED CONTENT

📄 Supporting Information

Average tumoroid size of hydrogel-encapsulated MDA PCa 183 and 118b cells over time. Cleaved caspase-3 expression of docetaxel-treated cells. This material is available free of charge via the Internet at <http://pubs.acs.org>.

■ AUTHOR INFORMATION

Corresponding Author

*(M.C.F.-C.) E-mail: farachca@rice.edu. Phone: 713-348-5052.

Notes

The contents of this article are solely the responsibility of the authors and do not necessarily represent the official views of the National Institutes of Health.

The authors declare no competing financial interest.

ACKNOWLEDGMENTS

This research is in part supported by the National Institutes of Health Grants P01 CA098912, Prostate SPOR grant SP50 CA140388, the Cancer Prevention & Research Institute of Texas grant RP11055, and the David H. Koch Center for Applied Research in Genitourinary Cancers at The University of Texas MD Anderson Cancer Center. E.L.F. acknowledges funding support from the National University of Singapore-Overseas Graduate Scholarship.

REFERENCES

- (1) Jacobs, S. C. Spread of prostatic cancer to bone. *Urology* **1983**, *21* (4), 337–44.
- (2) Logothetis, C. J.; Navone, N. M.; Lin, S. H. Understanding the biology of bone metastases: key to the effective treatment of prostate cancer. *Clin. Cancer Res.* **2008**, *14* (6), 1599–602.
- (3) Begley, C. G.; Ellis, L. M. Drug development: Raise standards for preclinical cancer research. *Nature* **2012**, *483* (7391), 531–3.
- (4) Thalmann, G. N.; Sikes, R. A.; Wu, T. T.; Degeorges, A.; Chang, S. M.; Ozen, M.; Pathak, S.; Chung, L. W. LNCaP progression model of human prostate cancer: androgen-independence and osseous metastasis. *Prostate* **2000**, *44* (2), 91–103.
- (5) Tentler, J. J.; Tan, A. C.; Weekes, C. D.; Jimeno, A.; Leong, S.; Pitts, T. M.; Arcaroli, J. J.; Messersmith, W. A.; Eckhardt, S. G. Patient-derived tumour xenografts as models for oncology drug development. *Nat. Rev. Clin. Oncol.* **2012**, *9* (6), 338–50.
- (6) Gray, D. R.; Huss, W. J.; Yau, J. M.; Durham, L. E.; Werdin, E. S.; Funkhouser, W. K., Jr.; Smith, G. J. Short-term human prostate primary xenografts: an in vivo model of human prostate cancer vasculature and angiogenesis. *Cancer Res.* **2004**, *64* (5), 1712–21.
- (7) Toivanen, R.; Frydenberg, M.; Murphy, D.; Pedersen, J.; Ryan, A.; Pook, D.; Berman, D. M.; Australian Prostate Cancer BioResource; Taylor, R. A.; Risbridger, G. P. A preclinical xenograft model identifies castration-tolerant cancer-repopulating cells in localized prostate tumors. *Sci. Transl. Med.* **2013**, *5* (187), 187ra71.
- (8) Yoshida, T.; Kinoshita, H.; Segawa, T.; Nakamura, E.; Inoue, T.; Shimizu, Y.; Kamoto, T.; Ogawa, O. Antiandrogen bicalutamide promotes tumor growth in a novel androgen-dependent prostate cancer xenograft model derived from a bicalutamide-treated patient. *Cancer Res.* **2005**, *65* (21), 9611–6.
- (9) Siolas, D.; Hannon, G. J. Patient-derived tumor xenografts: transforming clinical samples into mouse models. *Cancer Res.* **2013**, *73* (17), 5315–9.
- (10) Gurski, L. A.; Jha, A. K.; Zhang, C.; Jia, X.; Farach-Carson, M. C. Hyaluronic acid-based hydrogels as 3D matrices for in vitro evaluation of chemotherapeutic drugs using poorly adherent prostate cancer cells. *Biomaterials* **2009**, *30* (30), 6076–85.
- (11) Gurski, L. A.; Xu, X.; Labrada, L. N.; Nguyen, N. T.; Xiao, L.; van Golen, K. L.; Jia, X.; Farach-Carson, M. C. Hyaluronan (HA) interacting proteins RHAMM and hyaluronidase impact prostate cancer cell behavior and invadopodia formation in 3D HA-based hydrogels. *PLoS One* **2012**, *7* (11), e50075.
- (12) Xu, X.; Gurski, L. A.; Zhang, C.; Harrington, D. A.; Farach-Carson, M. C.; Jia, X. Recreating the tumor microenvironment in a bilayer, hyaluronic acid hydrogel construct for the growth of prostate cancer spheroids. *Biomaterials* **2012**, *33* (35), 9049–60.
- (13) Burdett, E.; Kasper, F. K.; Mikos, A. G.; Ludwig, J. A. Engineering tumors: a tissue engineering perspective in cancer biology. *Tissue Eng., Part B* **2010**, *16* (3), 351–9.
- (14) Toole, B. P. Hyaluronan: from extracellular glue to pericellular cue. *Nat. Rev. Cancer* **2004**, *4* (7), 528–39.
- (15) Zheng Shu, X.; Liu, Y.; Palumbo, F. S.; Luo, Y.; Prestwich, G. D. In situ crosslinkable hyaluronan hydrogels for tissue engineering. *Biomaterials* **2004**, *25* (7–8), 1339–48.
- (16) Vanderhooft, J. L.; Alcoutlabi, M.; Magda, J. J.; Prestwich, G. D. Rheological properties of cross-linked hyaluronan-gelatin hydrogels for tissue engineering. *Macromol. Biosci.* **2009**, *9* (1), 20–8.
- (17) Ghosh, K.; Shu, X. Z.; Mou, R.; Lombardi, J.; Prestwich, G. D.; Rafailovich, M. H.; Clark, R. A. Rheological characterization of in situ cross-linkable hyaluronan hydrogels. *Biomacromolecules* **2005**, *6* (5), 2857–65.
- (18) Li, Z. G.; Mathew, P.; Yang, J.; Starbuck, M. W.; Zurita, A. J.; Liu, J.; Sikes, C.; Multani, A. S.; Efsthathiou, E.; Lopez, A.; Wang, J.; Fanning, T. V.; Prieto, V. G.; Kundra, V.; Vazquez, E. S.; Troncoso, P.; Raymond, A. K.; Logothetis, C. J.; Lin, S. H.; Maity, S.; Navone, N. M. Androgen receptor-negative human prostate cancer cells induce osteogenesis in mice through FGF9-mediated mechanisms. *J. Clin. Invest.* **2008**, *118* (8), 2697–710.
- (19) Allen, R. G.; Eisenberg, S. R.; Gray, M. L. Quantitative measurement of the biological response of cartilage to mechanical deformation. *Methods Mol. Med.* **1999**, *18*, 521–42.
- (20) Shen, X.; Kramer, R. H. Adhesion-mediated squamous cell carcinoma survival through ligand-independent activation of epidermal growth factor receptor. *Am. J. Pathol.* **2004**, *165* (4), 1315–29.
- (21) Kondo, J.; Endo, H.; Okuyama, H.; Ishikawa, O.; Iishi, H.; Tsujii, M.; Ohue, M.; Inoue, M. Retaining cell-cell contact enables preparation and culture of spheroids composed of pure primary cancer cells from colorectal cancer. *Proc. Natl. Acad. Sci. U.S.A.* **2011**, *108* (15), 6235–40.
- (22) Karlou, M.; Lu, J. F.; Wu, G.; Maity, S.; Tzelepi, V.; Navone, N. M.; Hoang, A.; Logothetis, C. J.; Efsthathiou, E. Hedgehog signaling inhibition by the small molecule smoothened inhibitor GDC-0449 in the bone forming prostate cancer xenograft MDA PCa 118b. *Prostate* **2012**, *72* (15), 1638–47.
- (23) Massie, C. E.; Lynch, A.; Ramos-Montoya, A.; Boren, J.; Stark, R.; Fazli, L.; Warren, A.; Scott, H.; Madhu, B.; Sharma, N.; Bon, H.; Zecchini, V.; Smith, D. M.; Denicola, G. M.; Mathews, N.; Osborne, M.; Hadfield, J.; Macarthur, S.; Adryan, B.; Lyons, S. K.; Brindle, K. M.; Griffiths, J.; Gleave, M. E.; Rennie, P. S.; Neal, D. E.; Mills, I. G. The androgen receptor fuels prostate cancer by regulating central metabolism and biosynthesis. *EMBO J.* **2011**, *30* (13), 2719–33.
- (24) Heinlein, C. A.; Chang, C. Androgen receptor in prostate cancer. *Endocrine Rev.* **2004**, *25* (2), 276–308.
- (25) Gelmann, E. P. Molecular biology of the androgen receptor. *J. Clin. Oncol.* **2002**, *20* (13), 3001–15.
- (26) Rathkopf, D.; Scher, H. I. Androgen receptor antagonists in castration-resistant prostate cancer. *Cancer J.* **2013**, *19* (1), 43–9.
- (27) Gillet, J. P.; Calcagno, A. M.; Varma, S.; Marino, M.; Green, L. J.; Vora, M. I.; Patel, C.; Orina, J. N.; Eliseeva, T. A.; Singal, V.; Padmanabhan, R.; Davidson, B.; Ganapathi, R.; Sood, A. K.; Rueda, B. R.; Ambudkar, S. V.; Gottesman, M. M. Redefining the relevance of established cancer cell lines to the study of mechanisms of clinical anticancer drug resistance. *Proc. Natl. Acad. Sci. U.S.A.* **2011**, *108* (46), 18708–13.
- (28) Zhu, M. L.; Horbinski, C. M.; Garzotto, M.; Qian, D. Z.; Beer, T. M.; Kyprianou, N. Tubulin-targeting chemotherapy impairs androgen receptor activity in prostate cancer. *Cancer Res.* **2010**, *70* (20), 7992–8002.
- (29) Daniel, V. C.; Marchionni, L.; Hierman, J. S.; Rhodes, J. T.; Devereux, W. L.; Rudin, C. M.; Yung, R.; Parmigiani, G.; Dorsch, M.; Peacock, C. D.; Watkins, D. N. A primary xenograft model of small-cell lung cancer reveals irreversible changes in gene expression imposed by culture in vitro. *Cancer Res.* **2009**, *69* (8), 3364–73.
- (30) Landis, M. D.; Lehmann, B. D.; Pietenpol, J. A.; Chang, J. C. Patient-derived breast tumor xenografts facilitating personalized cancer therapy. *Breast Cancer Res.* **2013**, *15* (1), 201.
- (31) Burdall, S. E.; Hanby, A. M.; Lansdown, M. R.; Speirs, V. Breast cancer cell lines: friend or foe? *Breast Cancer Res.* **2003**, *5* (2), 89–95.
- (32) Weiswald, L. B.; Richon, S.; Validire, P.; Briffod, M.; Lai-Kuen, R.; Cordelieres, F. P.; Bertrand, F.; Dargere, D.; Massonnet, G.;

Marangoni, E.; Gayet, B.; Pocard, M.; Bieche, I.; Poupon, M. F.; Bellet, D.; Dangles-Marie, V. Newly characterised ex vivo colospheres as a three-dimensional colon cancer cell model of tumour aggressiveness. *Br. J. Cancer* **2009**, *101* (3), 473–82.